The Colored Refresh Server for DRAM

Xing Pan, Frank Mueller
North Carolina State University, Raleigh, USA, *mueller@cs.ncsu.edu*

***Abstract*—Bounding each task's worst-case execution time (WCET) accurately is essential for real-time systems to determine if all deadlines can be met. Yet, access latencies to Dynamic Random Access Memory (DRAM) vary significantly due to DRAM refresh, which blocks access to memory cells. Variations further increase as DRAM density grows.**

This work contributes the "Colored Refresh Server" (CRS), a uniprocessor scheduling paradigm that partitions DRAM in two distinctly colored groups such that refreshes of one color occur in parallel to the execution of real-time tasks of the other color. By executing tasks in phase with periodic DRAM refreshes with opposing colors, memory requests no longer suffer from refresh interference. Experimental results confirm that refresh overhead is completely hidden and memory throughput enhanced.

I. Introduction

Dynamic Random Access Memory (DRAM) has been the memory of choice in embedded systems for many years due low cost combined with large capacity, albeit at the expense of volatility. As specified by the DRAM standards [1], [2], each DRAM cell must be refreshed periodically within a given refresh interval. The refresh commands are issued by the DRAM controller via the command bus. This mode, called auto-refresh, recharges all memory cells within the "retention time", which is typically 64ms for commodity DRAMs under 85°C [1], [2]. While DRAM is being refreshed, a memory space (i.e., a DRAM rank) becomes unavailable to memory requests so that any such memory reference blocks the CPU pipeline until the refresh completes. Furthermore, a DRAM refresh command closes a previously open row and opens a new row subject to refresh [3], even though data of the old row may be reused (referenced) before and after the refresh. Hence, the delay suffered by the processor due to DRAM refresh includes two aspects: (1) the cost (blocking) of the refresh operation itself, and (2) reloads of the row buffer for data displaced by refreshes. As a result, the response time of a DRAM access depends on its point in time during execution relative to DRAM refresh operations.

Prior work indicated that system performance is significantly degraded by refresh overhead [4], [5], [6], [7], a problem that is becoming more prevalent as DRAMs are increasing in density. With growing density, more DRAM cells are required per chip, which must be refreshed within the same retention time, i.e., more rows need to be refreshed within the same refresh interval. This increases the cost of a refresh operation and thus reduces memory throughput. Even with conservative estimates of DRAM growth in density for future DRAM technology, the cost of one refresh operation, $tRFC$, exceeds 1 micro-second at 32 Gb DRAM size, and the loss in DRAM throughput caused by refreshes reaches nearly 50% at 64 Gb [4]. Some work focuses on reducing DRAM refresh latencies from both hardware and software angles. Although the DRAM refresh impact can be reduced by some proposed hardware solutions [8], [9], [10], [11], such solutions take a long time before they become widely adopted. Hence, other works seek to assess the viability of software solutions by lowering refresh overhead via exploiting inter-cell variation in retention time [4], [12], reducing unnecessary refreshes [13], [14], and decreasing the probability of a memory access interfering with a refresh [15], [7]. Fine Granularity Refresh (FGR), proposed by JeDEC's DDR4 specification, reduces refresh delays by trading off refresh latency against frequency [2]. Such software approaches either heavily rely on specific data access patterns of workloads or have high implementation overhead. More significantly, none of them can hide refresh overhead.

For real-time systems, the refresh problem is even more significant. Bounding the worst-case execution time (WCET) of a task's code is key to assuring correctness under schedulability analysis, and only static timing analysis methods can provide safe bounds on the WCET [16]. Due to the asynchronous nature of refreshes relative to task schedules and preemptions, none of the current analysis techniques tightly bound the effect of DRAM refreshes as a blocking term on response time. Atanassov and Puschner [17] discuss the impact of DRAM refresh on the execution time of real-time tasks and calculate the maximum possible increase of execution time due to refreshes. However, this bound is too pessimistic (loose): If the WCET or the blocking term were augmented by the maximum possible refresh delay, many schedules would become theoretically infeasible, even though executions may meet deadlines in practice. Furthermore, as the refresh overhead almost increases approximately linearly with growing DRAM density, it quickly becomes untenable to augment the WCET or blocking term by ever increasing refresh delays for future high density DRAM. Although Bhat et al. make refreshes predictable and reduce preemption due to refreshes by triggering them in software instead of hardware auto-refresh [3], the cost of refresh operations is only considered, but cannot be hidden. Also, a task cannot be scheduled under Bhat if its period is less than the execution time of a burst refresh.

This work contributes the "Colored Refresh Server" (CRS) to remove task preemptions due to refreshes and to hide DRAM refresh overhead. As a result, CRS makes real-time systems more predictable, particularly for high DRAM density. CRS exploits colored memory allocation to partition the entire

This work was supported in part by NSF grants 1239246,1329780,1525609 and 1813004.

memory space into two colors corresponding to two server tasks (simply called servers from here on) on a uniprocessor. Each real-time task is assigned one color and associated with the corresponding server, where the two servers have different static priorities. DRAM refresh operations are triggered by two tasks, each of which issues refresh commands to the memory of its corresponding server for a subset of a colors (DRAM ranks) using a burst refresh pattern. More significantly, by appropriately grouping real-time tasks into different servers, refreshes and competing memory accesses can be strategically co-scheduled so that memory reads/writes do not suffer from refresh interference. As a result, access latencies are reduced and memory throughput increases, which tends to result in schedulability of more real-time tasks. What is more, the overhead of CRS is small and remains constant irrespective of DRAM density/size. In contrast, auto-refreshed overhead keeps growing as DRAM density increases.

Contributions: (1) The impact of refresh delay under varying DRAM densities/sizes is assessed for real-time systems with stringent timing constraints. We observe that refresh overhead for an application is not easy to predict under standard auto-refresh. Furthermore, the losses in DRAM throughput and performance caused by refreshes quickly become unacceptable for real-time systems with high DRAM density.

(2) The Colored Refresh Server (CRS) for uniprocessors is developed to refresh DRAM via memory space coloring and shown to hide to schedule tasks via the server policy. refresh overhead almost entirely . hidden since a memory space is either being accessed or refreshed, but never both at the same time. Thus, regular memory accesses no longer suffer from refresh interference, i.e., the blocking effect of refreshes remains hidden in a safe manner.

(3) Experiments with real-time tasks confirm that both refresh delays are hidden and DRAM access latencies are reduced. Consequently, application execution times become more predictable and stable, even when DRAM density increases. An experimental comparison with DDR4's FGR shows that CRS exhibits better performance and higher task predictability.

(4) CRS is realized in software and can be implemented on commercial off-the-shelf (COTS) systems.

(5) Compared to previous work [3], CRS not only hides refresh overhead, but also feasibly schedules short tasks (period less than execution time of burst refresh) by refactoring them as "copy tasks".

(6) Our approach can be implemented with any real-time scheduling policy supported inside the CRS servers.

II. Background and Motivation

Today's computers predominantly utilize dynamic random access memory (DRAM), where each bit of data is stored in a separate capacitor within DRAM memory. To serve memory requests from the CPU, the memory controller acts as a mediator between the last-level cache (LLC) and DRAM devices (see Fig. 1) . Once memory transactions are received by a DRAM controller from its memory controller, these read/write requests are translated into corresponding DRAM commands and scheduled while satisfying the timing constraints of DRAM banks and buses. A DRAM controller is also called a node that governs DRAM memory organized into channels, ranks and banks (see Fig. 1).

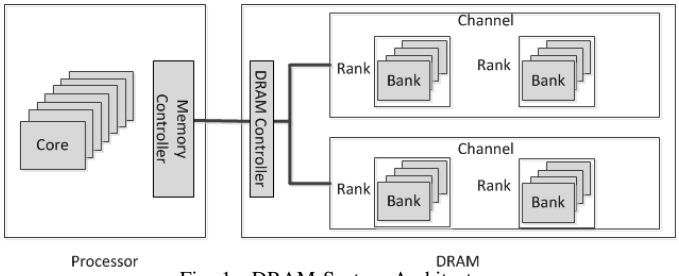

Fig. 1. DRAM System Architecture

A DRAM bank array is organized into rows and columns of individual data cells (see Fig. 2). To resolve a memory access request, the row containing the requested data needs to first be copied from the bank array into the row buffer. As a side effect, the old row in the buffer is closed ("precharge") incurring a Row Precharge delay, tRP, and the new row is opened ("activate") incurring a Row Access Strobe delay, $tRAS$. This is called a row buffer miss. Once loaded into the row buffer and opened, accesses of adjacent data in a row due to spatial locality incur just a Column Access Strobe penalty, $tCAS$ (row buffer hit), which is much faster than $tRP + tRAS$.

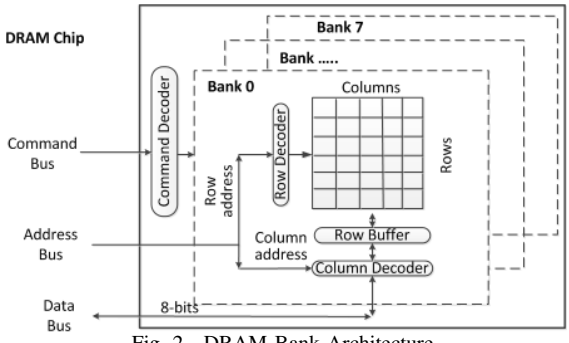

Fig. 2. DRAM Bank Architecture

A. Memory Space Partitioning

We assume a DRAM hierarchy with node, channel, rank, and bank abstraction. To partition this memory space, we obtained a copy of TintMalloc [18], a heap allocator that "colors" memory pages with controller (node) and bank affinity.

TintMalloc allows programmers to select one (or more) colors to choose a memory controller and bank regions disjoint from those of other tasks. DRAM is further partitioned into channels and ranks above banks. The memory space of an application can be chosen such that it conforms to a specific color. E.g., a real-time task can be assigned a private memory space based on rank granularity. When this task runs, it can only access the memory rank it is allocated to. No other memory rank will ever be touched by it. By design, there is a penalty for the first heap allocation request with a color under TintMalloc. This penalty only impacts the initialization phase. After a "first touch" page initialization, the latency of any subsequent accesses to colored memory is always lower than that of uncolored memory subject to buddy allocation (Linux default). Also, once the colored free list has been populated with pages, the initialization cost becomes constant for a stable

working set size, even for dynamic allocations/deallocation assuming they are balanced in size. Real-time tasks, after their initialization, experience highly predictable latencies for subsequent memory requests. Hence, a first coloring allocation suffices to amortize the overhead of initialization.

B. DRAM Refresh

Refresh commands are periodically issued by the DRAM controller to recharge all DRAM cells, which ensures data validity in the presence of electric leakage. A refresh command forces a read to each memory cell followed by a write-back without modification, which recharges the cell to its original level. The reference refresh interval of commodity DRAMs is 64ms under 85°C (185°F) or 32ms above 85°C, the so-called retention time, $tRET$, of leaky cells, sometimes also called refresh window, $tREFW$ [1], [2], [19], [20]. All rows in a DRAM chip need to be refreshed within $tRET$, otherwise data will be lost. In order to reduce refresh overhead, refresh commands are processed at rank granularity for commodity DRAM [21]. The DRAM controller can either schedule an automatic refresh for all ranks simultaneously (simultaneous refresh), or schedule automatic refresh commands for each rank independently (independent refresh). Whether simultaneous or independent, a successive area of multiple cells in consecutive cycles is affected by a memory refresh cycle. This area is called a "refresh bin" and contains multiple rows. The DDR3 specification [1] generally requires that 8192 automatic refresh commands are sent by the DRAM controller to refresh the entire memory (one command per bin at a time). Here, the refresh interval, $tREFI$, denotes the gap between two refresh commands, e.g., $tREFI = 7.8us$, i.e., $tREFW/8192$. The so-called refresh completion time, $tRFC$, is the refresh duration per bin. Auto-refresh is triggered in the background by the DRAM controller while the CPU executes instructions.

Memory ranks remain unavailable during a refresh cycle, $tRFC$, i.e., memory accesses (read and write operations) to this region will stall the CPU during a refresh cycle. The cost of a refresh operation is calculated as $tRFC/tREFI$. As density of DRAM chips grows, the size of each refresh bin becomes larger, i.e., it contains more rows. But the more rows in a refresh bin, the longer the refresh delay and memory blocking times become. The cost of a refresh operation, $tRFC$, is delimited by power constraints. Table I shows that The size of a refresh bin expands linearly with memory density so that $tRFC$ increases rapidly as DRAM density grows from 119ns at 1Gb to more than 1us at 32 Gb DRAM, even with conservative estimates of growth in density [4]. DRAM ranks can be refreshed in parallel under auto-refresh. However, the amount of unavailable memory increases when refreshing ranks in parallel. A fully parallel refresh blocks the entire memory space for $tRFC$. This blocking time not only decreases system performance, but can also result in deadline misses unless it is considered in a blocking term by all tasks.

Furthermore, a side effect of DRAM refresh is that a row buffer is first closed, i.e., its data is written back to the data array and any memory access is preempted. After the refresh completes, the original data is loaded back into the row buffer again, and the deferred memory access can continue. In other words, the row which contains data needs to be closed and re-opened due to interference between refresh and an in-flight memory access. As a result, an additional overhead of $tRP + tRAS$ is incurred to close and re-open rows since the refresh purges all buffers. This tends to result in additional row buffer misses and thus decreased memory throughput. Liu et al. [4] observe that the loss in DRAM throughput caused by refreshes quickly becomes untenable, reaching nearly 50% for 64 Gb DRAM. By considering both the cost of a refresh operation itself and the extra row close/re-open delay, DRAM refresh not only decreases memory performance, but also causes the response time of memory accesses to fluctuate. Due to the asynchronous nature of refreshes and task preemptions, it is hard to accurately predict and bound DRAM refresh delay. Depending on when a refresh command is sent to a bin (successive rows), two scheduling strategies exist: distributed and burst refresh (see Appendix A).

TABLE I
$tRFC$ FOR DIFFERENT DRAM DENSITIES (DATA FROM [1], [2], [4])

Chip Density	total rows	number of rows per bin	tRFC
1Gb	128K	16	$110ns$
2Gb	256K	32	$160ns$
4Gb	512K	64	$260ns$
8Gb	1M	128	$350ns$
16Gb	2M	256	$550ns$
32Gb	4M	512	$\geq 1us$
64Gb	8M	1K	$\geq 2us$

III. DESIGN

The core problem with the standard hardware-controlled auto-refresh is the interference between periodic refresh commands generated by the DRAM controller and memory access requests generated by the processor. The latter ones are blocked once one of the former is issued until the refresh completes. As a result, memory latency increases and becomes highly unpredictable since refreshes are asynchronous. The central idea of our approach is to remove DRAM refresh interference by memory partitioning (coloring). Given a real-time task set, we design a hierarchical resource model [22], [23], [24] to schedule it with two servers. To this end, we partition the DRAM space into two colors, and each server is assigned a colored memory partition. (We show in Sect. D of the appendix that two colors suffice, i.e., adding additional colors does not extend the applicability of the method, it would only make schedulability tests more restrictive.) By cooperatively grouping applications into two resource servers and appropriately configuring those servers (period and budget), we ensure that memory accesses can no longer be subject to interference by DRAM refreshes. Our approach can be adapted to any real-time scheduling policy supported inside the CRS servers. In this section, we describe the resource model, bound the timing requirements of each server, and analyze system schedulability.

A. Assumptions

We assume that a given real-time task set is schedulable with auto-refresh under a given scheduling policy (e.g., EDF or fixed priority), i.e., that the worst-case blocking time of refresh is taken into account. As specified by the DRAM standards [1], [2], the entire DRAM has to be refreshed within its retention time, $tRET$, either serially or in parallel for all K ranks. . We also assume hardware support for timer interrupts and memory controller interrupts (MC interrupts).

B. Task Model

Let us denote the set of periodic real-time tasks as $\mathcal{T} = \{T_1...T_n\}$, where each task, T_i, is characterized by (ϕ_i, p_i, e_i, D_i), or (p_i, e_i, D_i) if $\phi_i = 0$, or (p_i, e_i) if $p_i = D_i$ for a phase ϕ_i, a period p_i, (worst-case) execution time e_i, relative deadline D_i per job, task utilization $u_i = e_i/D_i$, and a hyperperiod H of $\mathcal{T}$. Furthermore, let
$tRET$ be the DRAM retention time,
L be the least common multiple of H and $tRET$, and
K be the number of DRAM ranks, and let k_i denote rank i.

C. DRAM Refresh Server Model

The Colored Refresh Server (CRS) partitions the entire DRAM space into two "colors", such that each color contains one or more DRAM ranks, e.g., $c_1(k_0, k_1...k_i)$, and $c_2(k_{i+1}, k_{i+2}...k_{K-1})$.

We build a hierarchical resource model (task server) [24], $S(W, A, c, p_s, e_s)$, with CPU time as the resource, where
W is the workload model (applications),
A is the scheduling algorithm, e.g., EDF or RM,
c denotes the memory color(s) assigned to this server, i.e., a set of memory ranks available for allocation,
p_s is the server period, and
e_s is the server execution time (budget). Notice that the base model [24] is compositional (assuming an anomaly-free processor design) and it has been shown that a schedulability test within the hyperperiod suffices for uniprocessors.

The refresh server can execute when
(i) its budget is not zero,
(ii) its available task queue is not empty, and
(iii) its memory color is not locked by a "refresh task" (introduced below). Otherwise, it remains suspended.

D. Refresh Lock and Unlock Tasks

We employ "software burst parallel refresh" [3] to refresh multiple DRAM ranks in parallel via the burst pattern (i.e., another refresh command is issued for the next row immediately after the previous one finishes , also see Appendix A with Fig. 11). In our approach, there are two "refresh lock tasks" (T_{rl1} and T_{rl2}) and two "refresh unlock tasks" (T_{ru1} and T_{ru2}), T_{rl1} and T_{ru1} surround the refresh for color c_1 and are allocated to server S_1 while T_{rl2} and T_{ru2} surround the refresh for color c_2 and are allocated by server S_2. The top-level task set $\mathcal{T}_\top$ of our hierarchical model thus consists of the two server tasks S_1 and S_2 plus another two tasks per color, with the highest priority, for refresh lock/unlock, T_{rl1} and T_{ru1} as well as T_{ru2} and T_{ru2}:

$\mathcal{T}_\top = \{S_1, S_2, T_{rl1}, T_{ru1}, T_{rl2}, T_{ru2}\}$.

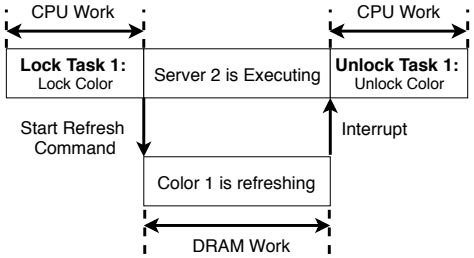

Fig. 3. Refresh Task with CPU Work plus DRAM Controller Work

When a refresh lock task is released (Fig. 3), the CPU sends a command to the DRAM controller to initiate parallel refreshes in a burst. Furthermore, a "virtual lock" is obtained for the colors subject to refresh. Due to their higher priority, refresh lock/unlock tasks preempt any server (if one was running) until they complete. Subsequently, the refresh lock task terminates so that a server task (of opposite color) can be resumed. In parallel, the "DRAM refresh work" is performed, i.e., burst refreshes are triggered by the controller. We use e_{r1} and e_{r2} to represent the duration of DRAM refresh per color $r1$ and $r2$, respectively. A CPU server resumes execution only if its budget is not exhausted, its allocated color is not locked, and some task in its server queue is ready to execute.

Once all burst refreshes have completed, an interrupt is triggered, which causes the CPU to call the refresh unlock task that unlocks the newly refreshed colors so that they become available again. This interrupt can be raised in two ways: (1) If the DRAM controller supports interrupt completion notification in hardware, it can be raised by the DRAM controller. (2) Otherwise, the length of a burst refresh, δ, can be measured and the interrupt can be triggered by imposing a phase of δ on the unlock task relative to the phase of the lock task of the same color. Interrupts are triggered at absolute times to reduce jitter (see Sect. IV). The overhead of this interrupt handler is folded into the refresh unlock task for schedulability analysis in the following. In practice, the cost of a refresh lock/unlock task is extremely small since it only programs the DRAM controller or handles the interrupt.

The periods of both the refresh lock and unlock task are $tRET$. The refresh lock tasks are released at $k * tRET$, while the refresh unlock tasks are released at $k * tRET + \delta$. The phases ϕ of T_{rl1} and T_{rl2} are $\frac{tRET}{2}$ and 0, respectively, i.e., memory ranks allocated to S_2 are refreshed first followed by those of S_1. Let us summarize:

$\mathcal{T}_\top = \{S_1, S_2, T_{rl1}, T_{ru1}, T_{rl2}, T_{ru2}\}$, where
$S_1 = (0, p_1, e_1, p_1), S_2 = (0, p_1, e_2, p_1)$,
$T_{rl1} = (tRET/2, tRET, e_{rl}, \delta), T_{rl2} = (0, tRET, e_{rl}, \delta)$,
$T_{ru1} = (tRET/2+\delta, tRET, e_{ru}, \delta), T_{ru2} = (\delta, tRET, e_{ru}, \delta)$.

The execution times e_{rl} and e_{ru} of the lock and unlock tasks are upper bounds on the respective interrupts plus programming the memory controllers for refresh and obtaining the lock for the former and just unlocking the the latter task, respectively. (They are also upper bounded by δ.) The

execution times e_1 and e_2 depend on the task sets of the servers covered later, while their deadlines are equal to their periods (p_1 and p_2). The task set $\mathcal{T}_\top$ can be scheduled statically as long as the lock and unlock tasks have a higher priority than the server tasks. A refresh unlock task is triggered by interrupt with a period of $tRET$. Since we refresh multiple ranks in parallel, the cost of refreshing one entire rank is the same as the cost of refreshing multiple ones. Furthermore, the cost of the DRAM burst refresh, δ, is small (e.g., less than $0.2ms$ for a 2Gb DRAM chip with 8 ranks) , and derived from the DRAM density according to Table I .

E. CRS Implementation

Consumption and Replenishment: The execution budget is consumed one time unit per unit of execution. The execution budget is set to e_s at time instants $k*p_s$, where $k \geq 0$. Unused execution budget cannot be carried over to the next period.

Scheduling: As described in Sec. III-D, the two refresh servers, S_1 and S_2, are treated as periodic tasks with their periods and execution times. We assign static priorities to servers and refresh tasks (lock and unlock). Instead of rate-monotonic priority assignment (shorter period, higher priority), static scheduling requires assignment of a strict fixed priority to each task (each server and each refresh task). The four refresh tasks receive the highest priority in the system. S_1 has the next highest priority and S_2 has a lower one than S_1. However, a server may only execute while its colors are unlocked. Tasks can be scheduled with any real-time scheduling policy supported inside the CRS servers, such as EDF, RM, or cyclic executive. During system initialization, we utilize the default hardware auto-refresh and switch to CRS once servers and refresh tasks have been released.

Example: Let there be four real-time tasks with periods and execution times of $T_1(16,4), T_2(16,2), T_3(32,8), T_4(64,8)$. DRAM is partitioned into 2 colors, c_1 and c_2, which in total contains 8 memory ranks (k_0 – k_7).

The four real-time tasks are grouped into two Colored Refresh Servers:
$S_1((T_1,T_2), RM, c_1(k_0,k_1,k_2,k_3), 16ms, 6ms)$ and
$S_2((T_3,T_4), RM, c_2(k_4,k_5,k_6,k_7), 16ms, 6ms)$.
In addition, refresh lock tasks T_{rl1} and T_{rl2} have a period of $tRET$ (64ms) and trigger refreshes for c_1 and c_2, respectively, i.e., T_{rl2} triggers refreshes for (k_4,k_5,k_6,k_7) with ϕ=0 while T_{rl1} triggers refreshes (k_0,k_1,k_2,k_3) with ϕ=32ms. Once refreshes have finished, the refresh unlock tasks T_{ru1} and T_{ru2} update corresponding memory colors to be available again.

Fig. 4 depicts the task execution for our CRS. Here, regular memory accesses from a processor of one color are overlaid with DRAM refresh commands of the opposite color, just by scheduling servers and refresh tasks according to their policies. We further observe that S_2 executes at time 32ms, even though S_1 has a higher priority than S_2. This is because color c_1 is locked by refresh task T_{rl1}. S_1 can preempt S_2 once c_1 is unlocked by T_{ru1}, i.e., after its DRAM refresh finishes.

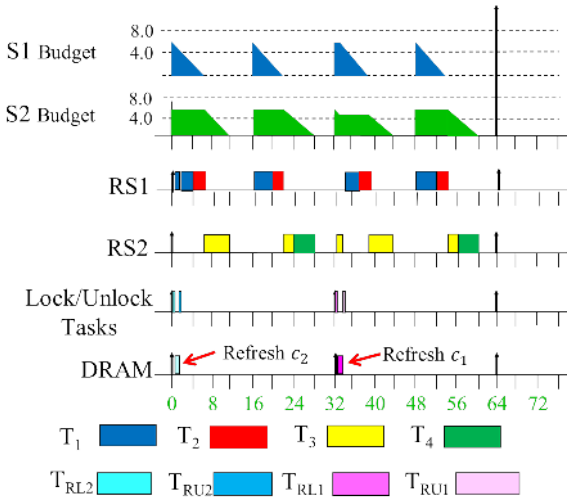

Fig. 4. Server scheduling example

F. Schedulability Analysis

In this section, we combine the analysis of the periodic capacity bound and the utilization bound (see Appendix C) to bound the response time, quantify the cost of CRS, and analyze the schedulability of entire system, including the servers and refresh lock/unlock tasks, i.e., T_{rl1} (0, $tRET$, e_{rl}, $tRET$), T_{rl2} ($tRET/2$, $tRET$, e_{rl}, $tRET$), T_{ru1} (δ, $tRET$, e_{ru}, $tRET$), T_{ru2} ($tRET/2+\delta$, $tRET$, e_{ru}, $tRET$), S_1 (p_1, e_1), and S_2 (p_2, e_2), where we assume that the two refresh lock tasks have the same execution time (e_{rl}), as do the two refresh unlock tasks (e_{ru}). Compared to auto-refresh, we build a hierarchical resource model (by selecting period, budget, and workload for both servers), which not only guarantees schedulability but also has a lower cost than the overhead of auto-refresh. As a result of removing DRAM refresh interference, our Colored Refresh Server outperforms auto-refresh.

As described in Sec. III-D, the refresh tasks, T_{rl1}, T_{rl2}, T_{ru1}, and T_{ru2}, have the highest priority, S_1 has the next highest priority, followed by S_2 with the lowest priority. To guarantee the schedulability of a real-time system with static priority scheduling, we require that
(1) each task satisfies the TDA (time demand analysis) requirement, and
(2) the total utilization does not exceed 1, i.e.,
$\frac{e_1}{p_1} + \frac{e_2}{p_2} + 2 * \frac{e_{rl}}{tRET} + 2 * \frac{e_{ru}}{tRET} \leq 1$.

For hierarchical resource models [24], S_1 and S_2 are treated as periodic tasks.

With auto-refresh, the maximum response time of S_1 is $r_{s1}^{(k)} = e_{s1} + b$, where $b = \lfloor \frac{r_{s1}^{(k-1)}}{tREFI} \rfloor * (tRFC + tRP + tRAS)$ represents the refresh overhead.

The maximum response time of S_2 is:
$r_{s2}^{(k)} = e_{s2} + \lceil \frac{r_{s2}^{(k-1)}}{p_{s1}} \rceil * e_{s1} + b$, where $b = \lfloor \frac{r_{s2}^{(k-1)}}{tREFI} \rfloor * (tRFC + tRP + tRAS)$ represents the refresh overhead.

With our CRS, S_1 and S_2 are co-scheduled with the refresh lock and unlock tasks. The maximum response time of S_1 is $r_{s1}^{(m)} = e_{s1} + 2 * \lceil \frac{r_{s1}^{(m-1)}}{tRET} \rceil * (e_{rl} + e_{ru}) + \epsilon_1$,

where ϵ_1 is the refresh overhead that cannot be hidden by our CRS, which is
$\epsilon_1 = \sum_{n,k} \gamma$ for $n \in [0, L/p_2]$ and $k \in [0, L/tRET]$; also
$\gamma = e_{r1}$ if
(1) $(m+1)*p_1 > p_{rl1}*k > m*p_1$ and $p_{rl1}*k - p_1*m \leq r_{s1}^m$
(2) $(n+1)*p_2 > p_{rl1}*k > n*p_2$ and $p_{rl1}*k - p_2*n \geq r_{s2}^n$;
otherwise, $\gamma = 0$.

The maximum response time of S_2 is:
$r_{s2}^{(n)} = e_{s2} + \lceil \frac{r_{s2}^{(n-1)}}{p_{s1}} \rceil * e_{s1} + 2 * \lceil \frac{r_{s2}^{(k-1)}}{tRET} \rceil * (e_{rl} + e_{ru}) + \epsilon_2$,
where ϵ_2 is the refresh overhead that cannot be hidden by our CRS, which is
$\epsilon_2 = \sum_{m,k} \gamma$ for $m \in [0, L/p_1]$ and $k \in [0, L/tRET]$; also
$\gamma = e_{r2}$ if
(1) $(m+1)*p_1 > p_{rl2}*k > m*p_1$ and $p_{rl2}*k - p_1*m \geq r_{s1}^m$
(2) $(n+1)*p_2 > p_{rl2}*k > n*p_2$ and $p_{rl2}*k - p_2*n \leq r_{s2}^n$;
otherwise, $\gamma = 0$.

As defined in Sec. III-D, e_{r1} and e_{r2} represent the execution time of burst refreshes for the corresponding colors, respectively. r_{s1}^m and r_{s2}^n can be calculated by response time analysis under fixed-priority assignment. As we showed above, the periods of both T_{rl1} and T_{rl2} are the DRAM retention time, i.e., $p_{rl1} = p_{rl2} = tRET$.

This shows that overhead is only incurred when a refresh task is released but its corresponding server (accessing the opposite color) is not ready to execute. Here, the overhead of refresh operations cannot be hidden. But this overhead is a small fraction of the entire DRAM refresh cost. Besides, it is predictable and quantifiable. The refresh overheads, ϵ_1 and ϵ_2, under CRS can be optimized as discussed next.

Let us assume a task set is partitioned into two groups, each associated with its own server. The servers with periods p_1 and p_2 each have a periodic capacity and utilization bound that can be calculated (shown in Appendix C). For server S_1 and S_2, let PCB_1 and PCB_2 denote their periodic capacity bounds, while UB_1 and UB_2 denote their utilization bounds.

The following algorithms find the lowest refresh overhead for each server. Algorithm 3 searches the entire range of available budgets and uses Algorithm 4 to quantify the refresh overhead. This search, which considers all permutations, is performed off-line, i.e., it does not incur overhead during real-time task execution.

With Algorithms 3 and 4, our CRS reduces the refresh overhead by selecting appropriate periods and budgets for each server. Compared to the response time under auto-refresh, CRS obtains a lower response time due to reduced refresh overhead, and requirement (1) is satisfied. We further assume that the execution times of refresh lock/unlock tasks (T_{rl1}, T_{rl2}, T_{ru1} and T_{ru2}) are identical (and known to be very small in practice). Since refresh tasks issue refresh commands in burst mode, CRS does not result in additional row buffer misses, i.e., e_{r1} and e_{r2} do not need to consider extra tRP or $tRAS$ overheads, which makes them smaller than their corresponding overheads under auto-refresh [3], i.e., requirement (2) is satisfied. Finally, our CRS not only bounds the response time of each server, but also guarantees system schedulability.

Algorithm 1 Optimize Refresh Overhead

```
Input: Two given workloads, W_1, W_2, of servers S_1, S_2, respectively
for p_1 in (0, hyperperiod of W_1] do
    for p_2 in (0, hyperperiod of W_2] do
        for e_1 in [PCB_1 * p_1, p_1] do
            for e_2 in [PCB_2 * p_2, p_2] do
                Calc. UB_1 using (p_1,e_1), UB_2 using (p_2,e_2), Appendix C
                if sum_{T_i in W_1} u_i <= UB_1 and sum_{T_j in W_2} u_j <= UB_2 then
                    for m in [0, L/p_1] do
                        ε_1 = Refresh_Overhead(1, m, (p_1, e_1), (p_2, e_2))
                        calculate r_{s1}^m
                        if r_{s1}^m >= p_1 then
                            break
                        end if
                        TotalCost_1 += ε_1
                    end for
                    for n in [0, L/p_2] do
                        ε_2 = Refresh_Overhead(2, n, (p_1, e_1), (p_2, e_2))
                        calculate r_{s2}^n
                        if r_{s2}^n >= p_2 then
                            break
                        end if
                        TotalCost_2 += ε_2
                    end for
                    if sum_{i=1}^{2} TotalCost_i < min_overhead then
                        budget_1 = e_1
                        budget_2 = e_2
                        min_overhead = TotalCost_1 + TotalCost_2
                    end if
                end if
            end for
        end for
    end for
end for
return budget_1 and budget_2
```

For a "short task", there is extra overhead under CRS due to the task copy cost (see Appendix B). The cost ($datasize * bandwidth$) can be folded into the response time of one sever if it has a copy task. However, the discussion in Appendix H shows that the cost of task copying is much less than the delay incurred on real-time tasks by a refresh, i.e., a "short task" can be scheduled under our CRS.

IV. Implementation

CRS has been implemented in an environment of three components, a CPU simulator, a scheduler combined with a coloring tool, and a DRAM simulator. SimpleScalar 3.0 [25] simulates the execution of an application and generates its memory traces. Memory traces are recorded to capture last-level cache (LLC) misses, i.e., from the L2 cache in our case. This information includes request intervals, physical address, command type, command size, etc. Each LLC miss results in a memory request (memory transaction) from processor to DRAM (see Fig. 5). The red/solid blocks and lines represent the LLC misses during application execution. The memory transactions of different applications are combined by a hierarchical scheduler according to scheduling policies (e.g., the priority of refresh tasks and servers at the upper level and task priorities within servers at the lower level). Furthermore, each memory transaction's physical address is colored based on the coloring policy (see "coloring tool" in Appendix E).

After scheduling and coloring, the memory traces are exposed to the DRAM simulator, RTMemController [26], to

Algorithm 2 Refresh_Overhead

```
Input:index, i, (p1, e1), (p2, e2)
for k in [0, L/tRET] do
    if index==1 then
        for n in [0, L/p2] do
            if (i+1)*p1 > tRET*k > i*p1 and
                (n+1)*p2 > tRET*k > n*p2 then
                calculate r^i_s1 and r^n_s2
                if tRET*k − p1*i ≤ r^i_s1 and
                    tRET*k − p2*n ≥ r^n_s2 then
                    return e_r1
                else
                    return 0
                end if
            end if
        end for
    end if
    if index==2 then
        for m in [0, L/p1] do
            if (m+1)*p1 > tRET*k > m*p1 and
                (i+1)*p2 > tRET*k > i*p2 then
                calculate r^m_s1 and r^i_s2
                if tRET*k − p1*m ≤ r^m_s1 and
                    tRET*k − p2*i ≥ r^i_s2 then
                    return e_r2
                else
                    return 0
                end if
            end if
        end for
    end if
end for
```

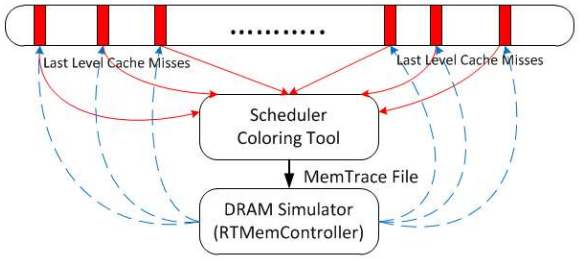

Fig. 5. System Architecture

analyze the DRAM performance. All memory transactions of the trace are scheduled by RTMemController, and their execution times are calculated. Instead of using fixed memory latencies for every task, which is the default, we enhanced SimpleScalar to consider the average execution time of each task's memory transactions analyzed by RTMemController over all LLC misses, which includes the DRAM refresh overhead. At last, the result of RTMemController (execution time of each memory transaction) is fed back to SimpleScalar to determine the application's overall execution time. This models the execution time of each real-time application, including its DRAM performance per memory access.

RTMemController is a back-end architecture for real-time memory controllers and was originally designed for DDR3 SDRAMs using dynamic command scheduling. We extended RTMemController to support burst refresh and DDR4 Fine Granularity Refresh (FGR). The performance of DRAM is analyzed by the enhanced RTMemController, which schedules the DRAM refresh commands at rank granularity.

The simulation environment also supports generation of an interrupt triggered by the DRAM controller when the bursts of a refresh task complete. Should a DRAM controller not support such an interrupt signal upon refresh completion, one can utilize a second timer. The refresh tasks are already triggered by a first periodic timer, say at time t. Once all DRAM refreshes have been issued by a refresh task, an absolute timer is installed for $t + tRFC$ (adding the refresh blocking time) to trigger the handler that unlocks the colors subject to refresh.

Color locks are implemented as attributes for scheduling at the top level, i.e., a flag per color suffices. Such a flag is set for colors of a refresh task before this refresh task is dispatched, and the flag is cleared inside the handler invoked upon refresh completion. We referred to a "virtual" lock earlier since the mechanism resembles a lock in terms of resource allocation for schedulability analysis. However, it cannot be implemented via a lock since a server task, if it obtained a lock, could not release it when interrupted by a refresh task. Instead, the refresh task would have to steal this lock, which is typically not supported by any API. Since we are implementing low-level scheduling directly, our flag solution is not only much easier to realize, it also has lower overhead as neither atomic instructions nor additional queues are required.

Discussion: This paper shows that the refresh overhead of a periodic real-time task set on a single processor can be hidden by our CRS. CRS could be generalized to multicore platforms under partitioned parallel scheduling of tasks with respect to cores, but the analysis would have to be revised beyond the hyperperiod as our base model [24] assumes a uniprocessor, whereas multicore schedules with task offsets may only reach a fixpoint after multiple hyperperiods [27]. Nonetheless, CRS could simply schedule the subset of tasks associated with the partition of a given core using CRS' hierarchical server model on a per-core basis, where servers receive different memory colors to guarantee when their allocated colors are not being refreshed while a server executes.

We evaluate our approach via hardware simulation, but software refresh control has been demonstrated on different hardware platforms [3], and CRS could be implemented with similar software refresh controls on such platforms (with some engineering overhead). DRAM refreshes are synchronous with the processor clock (if the clock is fixed) and can, in fact, optionally be disabled for a subset of ranks on contemporary single- and multi-core systems [28]. Furthermore, the phase when a per-rank hardware refresh starts could be reverse engineered by monitoring access latencies during the initialization of a CRS-controlled system on these platforms.

V. Evaluation Framework

The experimental evaluation assesses the performance of CRS relative to standard DRAM auto-refresh in four experiments. The first investigates the memory performance enhancements of CRS. The second illustrates how CRS hides the refresh delay instead of inflating execution times and guarantees the schedulability of real-time system. The third and fourth compare CRS with DDR4 Fine Granularity Refresh (FGR) and previous work, respectively.

We assess the Malardalen WCET benchmark programs [29] atop SimpleScalar 3.0 [25] combined with RTMemController [30]. The processor is configured with split data and instruction caches of 16KB size each, a unified L2 cache of 128KB size, and a cache line size of 64B. The memory system is a JEDEC-compliant DDR3 SDRAM (DDR3-1600G) with adjustable memory density (1Gb, 2Gb, 4Gb, 8Gb, 16Gb, 32Gb and 64Gb). The DRAM retention time, $tRET$, is 64 ms. Furthermore, there are 8 ranks, i.e., $K = 8$, and one memory controller per DRAM chip. (The approach requires a minimum of two ranks, which even small embedded systems tend to provide.) Refresh commands are issued by memory controllers at rank granularity.

TABLE II
REAL-TIME TASK SET

Application	Period	Execution Time
cnt	20ms	3ms
compress	10ms	1.2ms
lms	10ms	1.6ms
matmult	40ms	10ms
st	8ms	2ms

Multiple Malardalen applications are scheduled as real-time tasks under both CRS (hierarchical scheduling of refresh tasks plus servers and then real-time tasks within servers) and auto-refresh (single-level priority scheduling). Execution times and periods (deadlines) per Malardalen task are shown in Table II. Here, the base for execution time is an ideal one without refreshes. This ideal method is infeasible in a practice, but it provides a lower bound and allows us to assess how close a scheme is to this bound. The real-time task set shown in Table II can be scheduled under either a dynamic priority policy (e.g., EDF) or a static priority policy (e.g., RM and DM). We assess EDF due to space limitations, but CRS also works and obtains better performance than auto-refresh under static priority scheduling.

The task set in Table II has a hyperperiod of 40ms, and is schedulable under EDF without considering refresh overhead. CRS segregates each Malardalen application into one of the two servers. As shown in Sec.III-F, Algorithms 3 and 4 assist in finding a partition with minimal refresh overhead. There may be multiple best configurations under CRS, but we only assess experiments with one of them due to symmetry.

We employ two servers (S_1 and S_2) and refresh tasks (T_{rl1}, T_{rl2}, T_{ru1} and T_{ru2}). Applications "cnt", "lms" and "st" are assigned to S_1 with 4ms periods and a 2.4ms budget, while application "compress" and "matmult" belong to S_2 with 4ms periods and a 1.6ms budget. The entire memory space is equally partitioned into 2 colors (c_1 and c_2), i.e., the 8 DRAM ranks comprise 2 groups with 4 ranks each. TintMalloc [18] ensures that tasks of one server only access memory of one color, i.e., tasks in S_1 only allocate memory from the 4 ranks belonging to c_1 while tasks in S_2 only allocate from c_2. Furthermore, memory within c_1 and c_2 is triggered by T_{rl1} and T_{rl2} to be refresh by the burst pattern. The memory space is locked, and the server allocated to this space/color is prevented to execute during refresh until it is unlocked by T_{ru1} and T_{ru2} when all refresh operations finish. The periods of all refresh tasks (T_{rl1}, T_{rl2}, T_{ru1} and T_{ru2}) are equal to the DRAM retention time $tRET$ (64ms), and their phases are 32ms and 0 for T_{rl1} and T_{rl2}, respectively.

VI. EXPERIMENTAL RESULTS

Fig. 6 shows the memory access latency (y-axis) of auto-refresh normalized to that of CRS for all benchmarks at different DRAM densities (x-axis). The red/solid line inside the boxes indicates the median while the green/dashed line represents the average across the 5 tasks. The "whiskers" above/below the box indicate the maximum and minimum.

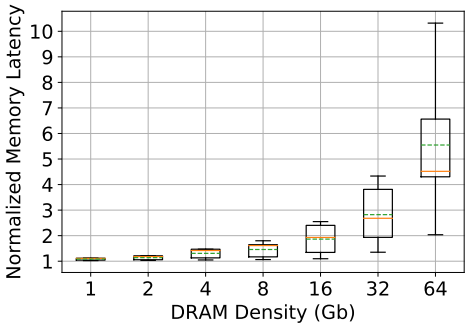

Fig. 6. Memory Latency of Auto-Refresh Normalized to CRS

We observe that CRS obtains better memory performance than auto-refresh, i.e., CRS reduces the memory latency due to refresh stalls for all DRAM densities. While auto-refresh suffers a small latency penalty at low DRAM density (8.34% on avg. at 1Gb density), this increases rapidly with density up to an unacceptable level (e.g., the average memory latency of auto-refresh increases by 455% relative to CRS at 64Gb). CRS avoids any latency penalty because memory requests of a real-time task do not (and cannot) interfere with any DRAM refresh since memory assigned to a server is not refreshed while the server executes. When this memory subspace needs to be refreshed, the respective server is suspended so that the other server may execute, which accesses memory of opposite color (not subject to refresh). In short, CRS co-schedules servers and refresh tasks such that any memory subspace can either be accessed by a processor or refreshed by the DRAM controller, but not by both at the same time. Hence, real-time tasks do not suffer from refresh overhead/blocking.

Observation 1: CRS avoids the memory latency penalty of auto-refresh, which increases with memory density under auto-refresh.

Auto-refresh not only increases memory access latency, it also causes memory performance to highly fluctuate across applications. Fig. 6 shows that different tasks suffer different latency penalties dependent on their memory access patterns. E.g., for a density of 16Gb, "compress" suffers a 9.7% increased latency while "cnt" suffers more than 154% increased latency. With growing density, the refresh delay increases not only due to longer execution time of refresh commands, but also because the probability of interference with refreshes increases. Fig. 7 illustrates this by plotting the number of memory references suffering from interference (y-axis) by task

over the same x-axis as before. Memory requests of a task suffer from more refresh interference with growing density since longer refresh durations imply a higher probability of blocking specific memory accesses.

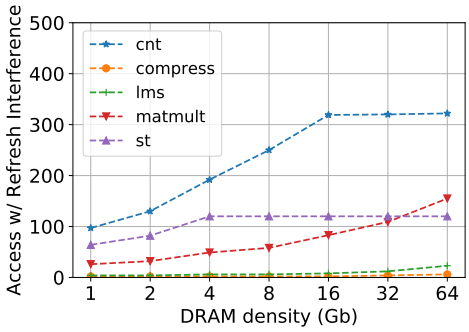

Fig. 7. Number of Memory Accesses with Refresh Interference

Observation 2: Auto-refresh results in high variability of memory access latency depending on memory access patterns and DRAM density while CRS hides this variability.

A. System Schedulability

Let us compare the execution time of each task under auto-refresh and CRS. Fig. 8 depicts the execution time of auto-refresh normalized to CRS (y-axis) over the same x-axis as before. We observe that execution times of tasks under auto-refresh exceed those under CRS since the latter avoids refresh blocking. Execution times increase rapidly with DRAM density under auto-refresh. E.g., refreshes increase execution times by 3.16% for 8Gb and by 22% at 64Gb for auto-refresh. The execution time of each application under CRS remains constant irrespective of DRAM density. Since there is no refresh blocking anymore, changing density has no effect on performance.

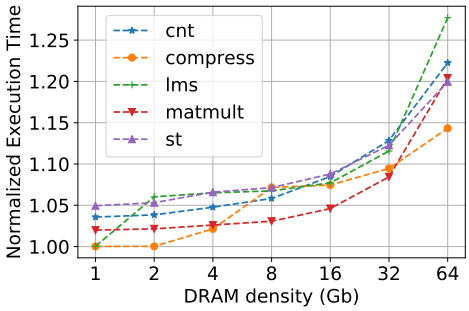

Fig. 8. Execution Time of Auto-Refresh Normalized to CRS

Fig. 9 depicts the overall system utilization factor (y-axis starting at 0.93) over DRAM densities (x-axis) of this real-time task set under different refresh methods. A lower utilization factor indicates better performance since the real-time system has more slack to guarantee schedulability. Auto-refresh experiences a higher utilization factor than CRS due to the longer execution times of tasks, which increases with density to the point where deadlines are missed (above factor 1.0) at 16, 32, and 64Gb.

In contrast, the utilization of CRS is lower and remains constant irrespective of densities. In fact, it is within 0.01% of the lower bound (non-refresh), i.e., scheduling overheads (e.g., due to preemption) are extremely low. Overall, CRS is superior because it co-schedules memory accesses and refreshes such that refresh interference is avoided.

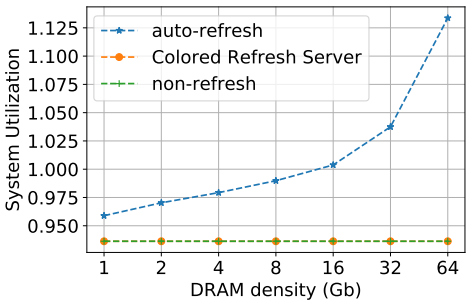

Fig. 9. System Utilization vs. DRAM Density

Observation 3: Compared to auto-refresh, CRS reduces the execution time of tasks and enhances system utilization by hiding refresh overheads, which increases predictability while preserving real-time schedulability. Furthermore, the performance of CRS remains stable and predictable irrespective of DRAM density while auto-refresh experiences increased overheads as density grows.

B. Fine Granularity Refresh

JEDECs DDR4 DRAM specification [2] introduces a Fine Granularity Refresh (FGR) that attempts to tackle increases in DRAM refresh overhead by creating a range of refresh options to provide a trade-off between refresh latency and frequency. We compared CRS with three FGR refresh options, namely the 1x, 2x, and 4x refresh modes. 1x is a direct extension of DDR2 and DDR3 refreshes. A certain amount of refresh commands are issued, and each command takes $tRFC$ time. The refresh interval, $tREFI$, of 1x is 7.8us [2]. 2x and 4x require refresh commands to be sent twice and four times as frequently, respectively. The interval, $tREFI$ is correspondingly reduced to 3.9us and 1.95us for 2x and 4x, respectively. More refresh commands mean fewer DRAM rows are refreshed per command, and, as a result, the refresh latencies, $tRFC$, for 2x and 4x are shorter. However, when moving from 1x to 2x and then 4x, $tREFI$ scales linearly, yet $tRFC$ does not. Instead, $tRFC$ decreases at a rate of less than 50% [5].

Fig. 12 depicts memory access latency (y-axis) normalized to CRS over DRAM densities (x-axis) for FGR 1x, 2x, and 4x. We observe that although 4x outperforms 1x and 2x, our approach uniformly provides the best performance and lowest memory access latency due to elimination of refresh blocking. After all, CRS hides the entire refresh operation while FGR reduces the refresh blocking time. Furthermore, the performance of FGR decreases with growing DRAM density. E.g., at 64Gb density, memory requests suffer an additional 17.6%, 20.7%, and 30.8% delay under FGR 4x, 2x and 1x, respectively, relative to CRS. This cost increases to 343.7%, 376.4%, and 454.8% at 64Gb. CRS, in contrast, hides refresh costs so that memory access latencies remain the same irrespective of DRAM densities.

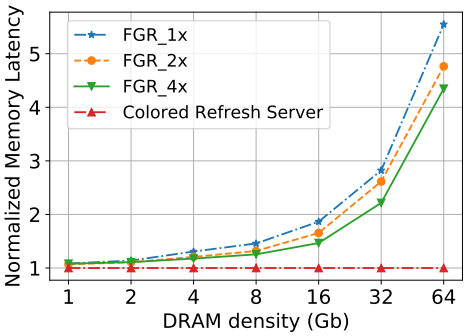

Fig. 10. Memory Latency under FGR Schemes Normalized to CRS

Observation 4: CRS exhibits better performance and higher task predictability than DDR4's FGR.

VII. Related Work

Contemporary DRAM specifications indicate increasing refresh latencies [1], [2], which prompted researcher to search for solutions. Recent works [21], [31], [32], [33], [6], [34] analyze DRAM refresh and quantify its penalty. The refresh overhead for DDR3+4 DRAM with high densities is discussed by Mukundan et al. [5]. While some focus on hardware to reduce the impact of DRAM refreshes [8], [9], [10], [11], others assess the viability of software solutions since hardware solutions take a long time before they become widely adopted.

Liu et al. [4] propose Retention-Aware Intelligent DRAM Refresh (RAIDR), which reduces refresh overhead by using knowledge of cell retention times. By exploiting the variation of DRAM cell retention time, RAIDR groups DRAM cells into several bins based on the measured minimum retention time cross all cells in a corresponding bin. Refresh overhead is reduced by RAIDR since rows are refreshed at different rates based on which bin they belong to. However, the retention time of a DRAM cell is sensitive to temperature, voltage, internal DRAM noise, manufacturer variability, and data access patterns. It may be risky to schedule refreshes at intervals beyond DRAM specifications as the retention time of cells is at least variable, if not unstable. RAPID [12] is a similar approach, where pages are sorted by their retention time and then allocated in this order to select pages with longer retention time first. Compared to CRS, these techniques reduce but cannot hide refresh blocking. RAPID not only suffers from similar risks as RAIDR, but also heavily relies on high memory locality to obtain better performance.

Smart Refresh [13] identifies and skips unnecessary refreshes by maintaining a refresh-needed counter. With this counter, a row that has been read or written since a refresh need not be refreshed again. Thus, memory performance is enhanced since the total number of refreshes is reduced. However, the performance of Smart Refresh heavily relies on knowledge about the data access pattern and has a high die space cost to maintain the refresh-needed counters. Liu et al. proposed Flikker [14], a selective DRAM refresh that uses a reference bit per row to record and determine if this row needs to be refreshed. Rows that are labeled "non-critical" will not be refreshed in order to reduce unnecessary refreshes. But the performance of Selective DRAM Refresh still heavily depends on the data access pattern. Our CRS is agnostic of data access patterns, and it does not require extra die space while its time overhead is very small. Bhati et al. [15] propose a new DRAM refresh architecture that combines refresh reduction techniques with the default auto-refresh. Unnecessary refreshes can be skipped, while ensuring that required refreshes are serviced. However, this approach does not hide refresh overhead completely, and it suffers from increased refresh latency for larger DRAM density/sizes.

Elastic Refresh [7] uses predictive mechanisms to decrease the probability of a memory access interfering with a refresh. Refresh commands are queued and scheduled when a DRAM rank is idle. This way, some interferences between memory accesses and refreshes can be avoided. However, as $tRFC$ increases with growing DRAM density, the probability of avoiding interferences decreases. In contrast, our CRS hides refresh delays for regular memory accesses under load. , and its performance is not affected by increasing DRAM density. Chang et al. [35] make hardware changes to the refresh scheduler inside the memory controller/DRAM subarrays. Kotra et al. [36] use LPDDR-technology for bank-partitioned scheduling without deadlines. Our work focuses on how real-time deadlines can be supported while hiding refresh via hierarchical scheduling in a server paradigm, including the assessment of overheads (lock/unlock) and the composition of tasks. Our work focuses on commodity DDR-technology, which is widely used in the embedded field and only supports rank partitions under refresh, but our methodology is equally applicable to LPDDR bank-partitioning (with its added flexibility). Other DRAM technology, e.g., RLDRAM [37], makes memory references more predictable but is subject to the same refresh blocking, i.e., CRS is directly applicable to them as well. Bhat et al. [3] make DRAM refresh more predictable. Instead of hardware auto-refresh, a software-initiated burst refresh is issued at the beginning of every DRAM retention period. After this refresh burst completes, there is no refresh interference for regular memory accesses during the remainder of DRAM retention time. But the memory remains unavailable during the refresh, and any stalls due to memory references at this time increase execution time. Although memory latency is predictable, memory throughput is still lower than CRS due to refresh blocking, i.e., CRS overlays (hides) refresh with computation. Furthermore, a task cannot be scheduled if its period is less than the duration of the burst refresh.

VIII. Conclusion

A novel uniprocessor scheduling server, CRS, is developed that hides DRAM refresh overheads via a software solution for refresh scheduling in real-time systems. Experimental results confirm that CRS increases the predictability of memory latency in real-time systems by eliminating blocking due to DRAM refreshes.

References

[1] JEDEC STANDARD, "DDR3 SDRAM SPECIFICATION," 2010.

[2] Standard, JEDEC, "DDR4 SDRAM," 2012.

[3] Balasubramanya Bhat and Frank Mueller, "Making DRAM refresh predictable," in *Euromicro Conference on Real-Time Systems*, 2010, pp. 145–154.

[4] Jamie Liu, Ben Jaiyen, Richard Veras, and Onur Mutlu, "RAIDR: Retention-aware intelligent DRAM refresh," *ACM SIGARCH Computer Architecture News*, vol. 40, no. 3, pp. 1–12, 2012.

[5] Janani Mukundan, Hillery Hunter, Kyu-hyoun Kim, Jeffrey Stuecheli, and José F Martínez, "Understanding and mitigating refresh overheads in high-density DDR4 DRAM systems," in *International Symposium on Computer Architecture*. ACM, 2013.

[6] Prashant Nair, Chia-Chen Chou, and Moinuddin K Qureshi, "A case for refresh pausing in DRAM memory systems," in *High Performance Computer Architecture*. IEEE, 2013, pp. 627–638.

[7] Jeffrey Stuecheli, Dimitris Kaseridis, Hillery C Hunter, and Lizy K John, "Elastic refresh: Techniques to mitigate refresh penalties in high density memory," in *International Symposium on Microarchitecture*. IEEE, 2010, pp. 375–384.

[8] Hongzhong Zheng, Jiang Lin, Zhao Zhang, Eugene Gorbatov, Howard David, and Zhichun Zhu, "Mini-rank: Adaptive DRAM architecture for improving memory power efficiency," in *International Symposium on Microarchitecture*. IEEE, 2008, pp. 210–221.

[9] Kevin Kai-Wei Chang, Donghyuk Lee, Zeshan Chishti, Alaa R Alameldeen, Chris Wilkerson, Yoongu Kim, and Onur Mutlu, "Improving DRAM performance by parallelizing refreshes with accesses," in *High Performance Computer Architecture*. IEEE, 2014, pp. 356–367.

[10] Joohee Kim and Marios C Papaefthymiou, "Dynamic memory design for low data-retention power," *Lecture notes in computer science*, 2000.

[11] Jan Reineke, Isaac Liu, Hiren D Patel, Sungjun Kim, and Edward A Lee, "Pret dram controller: Bank privatization for predictability and temporal isolation," in *Hardware/Software Codesign and System Synthesis*, 2011.

[12] Ravi Venkatesan, Stephen Herr, and Eric Rotenberg, "Retention-aware placement in DRAM (RAPID): Software methods for quasi-non-volatile DRAM," in *High-Performance Computer Architecture*, 2006, pp. 155–165.

[13] Mrinmoy Ghosh and Hsien-Hsin S Lee, "Smart refresh: An enhanced memory controller design for reducing energy in conventional and 3D die-stacked DRAMs," in *International Symposium on Microarchitecture*. IEEE, 2007, pp. 134–145.

[14] Song Liu, Karthik Pattabiraman, Thomas Moscibroda, and Benjamin G Zorn, "Flikker: saving DRAM refresh-power through critical data partitioning," *Architectural Support for Programming Languages and Operating Systems*, pp. 213–224, 2011.

[15] Ishwar Bhati, Zeshan Chishti, Shih-Lien Lu, and Bruce Jacob, "Flexible auto-refresh: enabling scalable and energy-efficient DRAM refresh reductions," in *International Symposium on Computer Architecture*, 2015.

[16] Joachim Wegener and Frank Mueller, "A comparison of static analysis and evolutionary testing for the verification of timing constraints," *Real-Time Systems*, 2001.

[17] Pavel Atanassov and Peter Puschner, "Impact of dram refresh on the execution time of real-time tasks," in *Proc. IEEE International Workshop on Application of Reliable Computing and Communication*, 2001.

[18] Xing Pan, Yasaswini Jyothi Gownivaripalli, and Frank Mueller, "Tint-malloc: Reducing memory access divergence via controller-aware coloring," in *International Parallel and Distributed Processing Symposium*. IEEE, 2016, pp. 363–372.

[19] Heesang Kim, Byoungchan Oh, Younghwan Son, Kyungdo Kim, Seon-Yong Cha, Jae-Goan Jeong, Sung-Joo Hong, and Hyungcheol Shin, "Characterization of the variable retention time in dynamic random access memory," *IEEE Transactions on Electron Devices*, 2011.

[20] Yuki Mori, Kiyonori Ohyu, Kensuke Okonogi, and R-I Yamada, "The origin of variable retention time in dram," in *Electron Devices Meeting*, 2005.

[21] Ishwar Bhati, Mu-Tien Chang, Zeshan Chishti, Shih-Lien Lu, and Bruce Jacob, "DRAM refresh mechanisms, penalties, and trade-offs," *IEEE Transactions on Computers*, vol. 65, no. 1, pp. 108–121, 2016.

[22] Xiang Feng and Aloysius K Mok, "A model of hierarchical real-time virtual resources," in *Real-Time Systems Symposium*, 2002.

[23] Giuseppe Lipari and Enrico Bini, "Resource partitioning among real-time applications," in *Euromicro Conference on Real-Time Systems*, 2003.

[24] Insik Shin and Insup Lee, "Periodic resource model for compositional real-time guarantees," in *IEEE Real-Time Systems Symposium*, 2003.

[25] D. Burger, T. Austin, and S. Bennett, "Evaluating future microprocessors: The simplescalar toolset," Tech. Rep. CS-TR-96-1308, University of Wisconsin - Madison, CS Dept., July 1996.

[26] Yonghui Li, Benny Akesson, and Kees Goossens, "Dynamic command scheduling for real-time memory controllers," in *Euromicro Conference on Real-Time Systems*. IEEE, 2014, pp. 3–14.

[27] Joël Goossens, Emmanuel Grolleau, and Liliana Cucu-Grosjean, "Periodicity of real-time schedules for dependent periodic tasks on identical multiprocessor platforms," *Real-Time Systems*, vol. 52, no. 6, pp. 808–832, Nov. 2016.

[28] Konstantinos Tovletoglou, Dimitrios S Nikolopoulos, and Georgios Karakonstantis, "Relaxing dram refresh rate through access pattern scheduling: A case study on stencil-based algorithms," in *Int'l Symp. on On-Line Testing and Robust System Design*, 2017.

[29] Jan Gustafsson, Adam Betts, Andreas Ermedahl, and Björn Lisper, "The mälardalen wcet benchmarks: Past, present and future," in *International Workshop on Worst-Case Execution Time Analysis (WCET),*, 2010.

[30] Y Li, B Akesson, and K Goossens, "Rtmemcontroller: Open-source wcet and acet analysis tool for real-time memory controllers," http://www.es.ele.tue.nl/rtmemcontroller/, 2014.

[31] Philip G Emma, William R Reohr, and Mesut Meterelliyoz, "Rethinking refresh: Increasing availability and reducing power in DRAM for cache applications," *IEEE micro*, pp. 47–56, 2008.

[32] Jamie Liu, Ben Jaiyen, Yoongu Kim, Chris Wilkerson, and Onur Mutlu, "An experimental study of data retention behavior in modern DRAM devices: Implications for retention time profiling mechanisms," in *International Symposium on Computer Architecture*. ACM, 2013.

[33] Kinam Kim and Jooyoung Lee, "A new investigation of data retention time in truly nanoscaled DRAMs," *IEEE Electron Device Letters*, pp. 846–848, 2009.

[34] Takeshi Hamamoto, Soichi Sugiura, and Shizuo Sawada, "On the retention time distribution of dynamic random access memory (dram)," *IEEE Transactions on Electron devices*, 1998.

[35] K. K. Chang, D. Lee, Z. Chishti, A. R. Alameldeen, C. Wilkerson, Y. Kim, and O. Mutlu, "Improving dram performance by parallelizing refreshes with accesses," in *International Symposium on High Performance Computer Architecture*, Feb 2014, pp. 356–367.

[36] Jagadish B. Kotra, Narges Shahidi, Zeshan A. Chishti, and Mahmut T. Kandemir, "Hardware-software co-design to mitigate dram refresh overheads: A case for refresh-aware process scheduling," *SIGPLAN Not.*, vol. 52, no. 4, pp. 723–736, Apr. 2017.

[37] M. Hassan, "On the off-chip memory latency of real-time systems: Is ddr dram really the best option?," in *IEEE Real-Time Systems Symposium*, Dec. 2018, pp. 495–505.

[38] Standard, JEDEC, "LPDDR3 SDRAM Specification," 2012.

APPENDIX

A. Refresh Mode and Scheduling Strategy

For commodity DDRx (e.g., DDR3 and DDR4), refresh operations are issued at rank granularity. A single refresh command for a given rank precharges all banks within this rank, which is called "All-Bank" refresh [21]. In contrast, recent LPDDRx DRAM [38] supports an enhanced "Per-Bank" mode to refresh cells at bank level while other banks in the same rank may be serviced. "Per-Bank" consumes more refresh time overall than "All-Bank" but achieves higher bank parallelism [15]. For each rank, a refresh counter maintains the address of the row to be refreshed and applies charges to the chip's row address lines. A timer then increments the refresh counter to step through the rows. Depending on when a refresh command is sent to a bin (successive rows), two scheduling strategies exist, namely distributed and burst refresh (see Fig. 11).

Distributed Refresh: A single refresh operation is performed periodically. Once all rows are refreshed, the refresh cycle is repeated by starting from the first row. As Fig. 11 shows, distributed refresh only schedules one automatic refresh every $tREFI$. All refreshes are sent by the DRAM controller and performed in hardware. Distributed refresh is currently the most common method. However, the response time of regular memory accesses varies over a wide time range due to the spread of refreshes, and due to the overhead incurred by closing the row buffer.

Burst refresh: A series of refresh cycles are performed back-to-back ($tREFI = 0$) until all rows have been refreshed. After that, the memory is available for accesses until the next refresh, which is issued after $tRET$, the DRAM retention time. As shown in Fig. 11, sequential refreshes are performed successively at the beginning of each $tRET$ period. Although burst refresh can reduce extra row buffer misses, the cost of refresh operations still decreases DRAM system performance. More importantly, a burst refresh results in long periods during which the memory is unavailable, which also affects task execution and results in longer memory latencies, yet such bursts occur less frequently. For real-time systems, a long memory blocking time may result in deadline misses, in particular if the period of a real-time task is short.

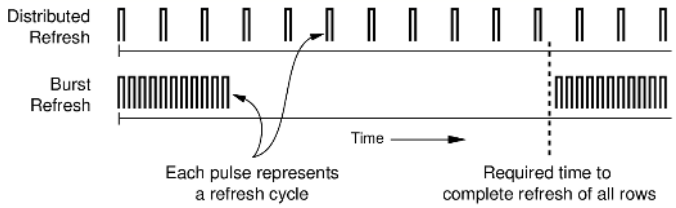

Fig. 11. DRAM Refresh Strategy

B. Copy Task

To schedule short tasks, we next propose the concept of a "copy task". A short task is defined as one whose period is less than the burst refresh cost. Such tasks are not schedulable in [3].

Our novel approach creates two instances of a task, the original one and a so-called "copy tasks". The two instances have identical control flow, but their data is referencing memory allocated from different colors so that the two instances belong to different servers. When a job of this task is released, our approach selects the instance to execute based on which server is running. Once one instance starts, its data is forwarded (copied) from another color if its previous instance had been allocated to a different color than the current one. Notice that differences in colors of consecutive instances can be determined statically over the entire hyperperiod, i.e., it is possible to perform this check statically so that the copy subroutine is triggered for exactly those instances prefixed by a different color instance. The trade-off between CRS's refresh hiding and the forwarding cost, calculated as $datasize * bandwidth$, is evaluated Appendix H.

C. Schedulability Analysis within a Server

In this section, we analyze the schedulability of tasks within a server by modeling the "Periodic Capacity Bound" and the "Utilization Bound". For each server, $S(W, A, c, p_s, e_s)$, we can bound the periodic capacity for its period and budget that guarantees the schedulability of workload W and scheduling algorithm A. Similarly, when characterizing its period, budget and scheduling algorithm, we determine a utilization bound for its workload W that guarantees the schedulability of this server. Let us derive the periodic capacity bounds and the utilization bounds for the EDF algorithm and the RM algorithm, respectively.

EDF: For our CRS, DRAM refresh operations are performed by the refresh tasks (lock and unlock), which are outside of the servers. As a result, there is no refresh overhead within each server.

The resource demand bound function [24] under EDF is:
$dbf(t) = \sum_{T_i \in W} \lfloor \frac{t}{p_i} \rfloor * e_i$

(i) Periodic Capacity Bound (PCB): For a sever with period p_s and budget e_s, its lowest supply bound function during t time units $lsbf(t)$ is [24]:
$lsbf(t) = \frac{e_s}{p_s} * (t - 2 * (p_s - e_s))$
In order to guarantee schedulability of tasks within a server, $\forall\ 0 < t \leq H : dbf(t) \leq lsbf(t)$, where H is the hyperperiod of tasks within this server.

$dbf(t) \leq lsbf(t) = \frac{e_s}{p_s} * (t - 2 * (p_s - e_s))$.

We have $PCB = \frac{e_s}{p_s}$, where
$e_s \geq \frac{\sqrt{(t-2p_s)^2 + 8p_s * dbf(t)} - (t - 2p_s)}{4}$.

(ii) Utilization Bound (UB): For a task set W, its utilization bound U_W can be calculated as $p' * U_W \leq lsbf(p')$ [24], where p' is the smallest period in task set W.

$U_W \leq \frac{lsbf(p')}{p'} = \frac{e_s}{p_s} * (\frac{p' - 2(p_s - e_s)}{p'}) = \frac{e_s}{p_s} * (1 - \frac{2(p_s - e_s)}{p'})$.

RM: The response time of a task is
$r_i^{(k)} = e_i + \sum_{T_k \in HP(W,T_k)} \lceil \frac{r_i^{(k-1)}}{p_k} \rceil * e_k$. As discussed before, there is no refresh overhead within each server.

(i) Periodic Capacity Bound (PCB): The linear service time bound function $ltbf(t)$ represents the upper bound of service time to supply t time units of a resource [24]:
$ltbf(t) = \frac{p_s}{e_s} * t + 2(p_s - e_s)$.

To guarantee schedulability of tasks within a server, e.g., for T_i, the service time to supply $r_i^{(k)}$ should be less than its period, p_i, i.e.,
$ltbf(r_i^{(k)}) = \frac{p_s}{e_s} * r_i^{(k)} + 2 * (p_s - e_s) \leq p_i$.

As a result, the periodic capacity bound (PCB) is $PCB = \frac{e_s}{p_s}$, where
$e_s \geq \frac{\sqrt{(p_i - 2p_s)^2 + 8 * p_s * r_i^{(k)}} - (p_i - 2p_s)}{4}$.

(ii) Utilization Bound (UB): For a task set W, its utilization bound, U_W, can be calculated as $U_W = \frac{e_s}{p_s} * (ln2 - \frac{p_s - e_s}{p'})$, where p' is the shortest period in the task set.

D. Two Colors Suffice

Our approach uses only two colors, which raises the question if more colors extend the applicability of our method. In short, the answer is no. We will sketch a proof in the following.

Let us assume an n-colored system with n servers $X_1 ... X_n$ with phases $i * tRET/n$ for X_i. Any such system can then be reduced to a $(n-1)$-colored set of servers $S_1 .. S_{n-1}$ as follows. Let $S_i = X_i$ for $1...n-1$. Let T_1 be a task of X_n. If T_1 never runs during S_i's refresh interval, we can simply assign it to T_i. If T_1 runs during multiple of S_i's refresh intervals, then we assign all instances of T_1 to S_1, except the ones that occur during S_1's refresh, which we assign as $T_1^{'}$ (a copy tasks) to S_2 (see Sect. B). This creates copy task overhead, but this overhead is so small (see last paragraph of appendix) that the extra overhead of context switches plus interrupts for lock/unlocks tasks of S_3 would likely be larger. The budget of X_n is distributed proportionately to the S_is that its tasks are assigned to. This process is repeated for all tasks of X_n. Further, any n-colored set of servers can be inductively reduced to a 2-colored server system using the constructive steps (essentially an algorithm) above.

E. Coloring Tool

To hide the refresh overhead for real-time systems, our approach requires that each task be assigned a memory color via colored memory allocation. We ported TintMalloc [18] to SimpleScalar so that it can select the color of physical addresses in memory. In the experiments, the entire DRAM is split into two colors corresponding to the two servers, and each application is assigned to one of them. We can adjust the number of ranks associated with one color, e.g., in order to meet an application's memory requirement. The TintMalloc tool takes as an input an application's memory trace and scans the physical addresses accessed. To color a memory space, the Rank_ID of each physical address is calculated, and it is checked if it belongs to the colors assigned to this application. In our case, the rank ID is determined by bits 15-17 of the physical address. If the Rank_ID does not match, these bits are set to the task's respective color. Otherwise, the physical address remains unchanged. Example: Consider a total of 8 ranks, let ranks 0-3 belong to color_1 while ranks 4-7 are in color_2. When an application is assigned to color_1, TintMalloc ensures that all its pages are in the 0-3 rank range by resetting bits 15-17 of the physical address (in the page range). To avoid duplicated physical addresses, TintMalloc's port not only changes the rank ID of the physical address, but also assigns this address to a new free page of the corresponding color. We further retain page locality of physical addresses, i.e., if two physical addresses originally reside in the same page, they still share the same page after coloring. Once applications are colored this way, all physical addresses of a trace belong to a particular memory segment (color), and a task only accesses this specific area as per coloring policy.

F. Algorithms to Assign Tasks to Servers

The following algorithms find the lowest refresh overhead for each server. Algorithm 3 searches the entire range of available budgets and uses Algorithm 4 to quantify the refresh overhead. This search, which considers all permutations, is performed off-line, i.e., it does not incur overhead during real-time task execution.

Algorithm 3 Optimize Refresh Overhead

```
Input: Two given workloads, W1, W2, of servers S1, S2, respectively
for p1 in (0, hyperperiod of W1] do
    for p2 in (0, hyperperiod of W2] do
        for e1 in [PCB1 * p1, p1] do
            for e2 in [PCB2 * p2, p2] do
                Calc. UB1 using (p1,e1), UB2 using (p2,e2), see Appendix C
                if sum_{Ti in W1} ui <= UB1 and sum_{Tj in W2} uj <= UB2 then
                    for m in [0, L/p1] do
                        e1 = Refresh_Overhead(1, m, (p1, e1), (p2, e2))
                        calculate r^m_s1
                        if r^m_s1 >= p1 then
                            break
                        end if
                        TotalCost1 += e1
                    end for
                    for n in [0, L/p2] do
                        e2 = Refresh_Overhead(2, n, (p1, e1), (p2, e2))
                        calculate r^n_s2
                        if r^n_s2 >= p2 then
                            break
                        end if
                        TotalCost2 += e2
                    end for
                    if sum_{i=1}^{2} TotalCost_i < min_overhead then
                        budget1 = e1
                        budget2 = e2
                        min_overhead = TotalCost1 + TotalCost2
                    end if
                end if
            end for
        end for
    end for
end for
return budget1 and budget2
```

With Algorithms 3 and 4, our CRS reduces the refresh overhead by selecting appropriate periods and budgets for each server.

G. Fine Granularity Refresh

JEDECs DDR4 DRAM specification [2] introduces a Fine Granularity Refresh (FGR) that attempts to tackle increases in DRAM refresh overhead by creating a range of refresh options to provide a trade-off between refresh latency and frequency. We compared CRS with three FGR refresh options, namely the 1x, 2x, and 4x refresh modes. 1x is a direct

Algorithm 4 Refresh_Overhead

```
Input:index, i, (p1, e1), (p2, e2)
for k in [0, L/tRET] do
    if index==1 then
        for n in [0, L/p2] do
            if (i+1)*p1 > tRET*k > i*p1 and
                (n+1)*p2 > tRET*k > n*p2 then
                calculate r^i_s1 and r^n_s2
                if tRET*k − p1*i ≤ r^i_s1 and
                    tRET*k − p2*n ≥ r^n_s2 then
                    return e_r1
                else
                    return 0
                end if
            end if
        end for
    end if
    if index==2 then
        for m in [0, L/p1] do
            if (m+1)*p1 > tRET*k > m*p1 and
                (i+1)*p2 > tRET*k > i*p2 then
                calculate r^m_s1 and r^i_s2
                if tRET*k − p1*m ≤ r^m_s1 and
                    tRET*k − p2*i ≥ r^i_s2 then
                    return e_r2
                else
                    return 0
                end if
            end if
        end for
    end if
end for
```

extension of DDR2 and DDR3 refreshes. A certain amount of refresh commands are issued, and each command takes $tRFC$ time. The refresh interval, $tREFI$, of 1x is 7.8us [2]. 2x and 4x require refresh commands to be sent twice and four times as frequently, respectively. The interval, $tREFI$ is correspondingly reduced to 3.9us and 1.95us for 2x and 4x, respectively. More refresh commands mean fewer DRAM rows are refreshed per command, and, as a result, the refresh latencies, $tRFC$, for 2x and 4x are shorter. However, when moving from 1x to 2x and then 4x, $tREFI$ scales linearly, yet $tRFC$ does not. Instead, $tRFC$ decreases at a rate of less than 50% [5].

Fig. 12 depicts memory access latency (y-axis) normalized to CRS over DRAM densities (x-axis) for FGR 1x, 2x, and 4x. We observe that although 4x outperforms 1x and 2x, our approach uniformly provides the best performance and lowest memory access latency due to elimination of refresh blocking. After all, CRS hides the entire refresh operation while FGR reduces the refresh blocking time. Furthermore, the performance of FGR decreases with growing DRAM density. E.g., at 64Gb density, memory requests suffer an additional 17.6%, 20.7%, and 30.8% delay under FGR 4x, 2x and 1x, respectively, relative to CRS. This cost increases to 343.7%, 376.4%, and 454.8% at 64Gb. CRS, in contrast, hides refresh costs so that memory access latencies remain the same irrespective of DRAM densities.

Observation 4: CRS exhibits better performance and higher task predictability than DDR4's FGR.

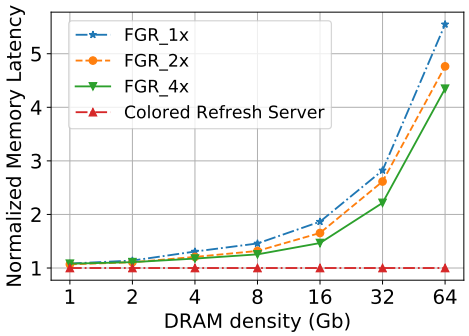

Fig. 12. Memory Latency under FGR Schemes Normalized to CRS

H. Comparison with Prior Work

Bhat et al. [3] utilized burst patterns to reduce refresh delay and increase timing predictability. We compare the performance of CRS with the "burst-refresh" policy of [3]. Fig. 13 depicts the memory access latency (y-axis) normalized to CRS under for different DRAM densities (x-axis) for three refresh schemes. We observe that burst-refresh has a better performance than standard auto-refresh since it reduces blocking by preempting lower priority tasks while refreshing. But it cannot reduce the cost of refresh operations, which by far exceeds the interference delay. As a result, the performance of burst-refresh still suffers as it decreases rapidly with growing DRAM density. In contrast, CRS not only incurs a constant preemption cost to issue the DRAM burst, but resumes one set of tasks while some set of ranks are refreshed. The other set of ranks are thus accessed by the resumed tasks, which effectively hides the cost of refresh. Hence, our approach outperforms burst-refresh. As mentioned before, memory access latencies remain constant under CRS irrespective of density.

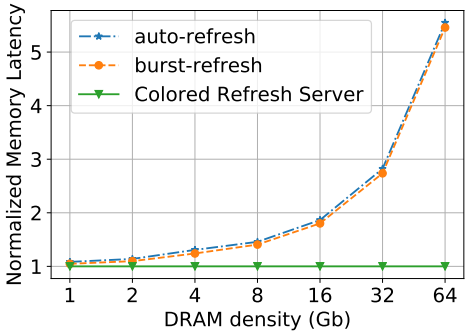

Fig. 13. Memory Latency per Refresh Scheme Normalized to CRS

In addition, a task cannot be scheduled under Bhat's approach [3] if its period is less than the execution time of a burst refresh. However, such a task can be scheduled under CRS by "task copying" (see Sec. B). The cost of task copying is extremely small, as quantified by $\frac{globalMem}{bandwidth}$. Here, $globalMem$ denotes the cumulative size of global variables that need to be copied from a current to the next job's memory space, while $bandwidth$ represents the memory bandwidth. We can determine if a short task benefits from task copying by comparing the copy cost to the overhead it would suffer under refresh-incurred blocking instead:
$\frac{globalMem}{bandwidth} \leq \frac{tRFC}{tRFI} * e$, where e is the task's execution time

and $\frac{tRFC}{tRFI} * e$ represents the overhead due to refresh (upper bound) that would have to be considered in a blocking term during schedulability analysis.

Example: The cost of one refresh operation is $tRFC = 350ns$, and the length of a refresh interval is $tRFI = 7.8us$ for 8Gb DRAM density, which is common in commercial off-the-shelf embedded systems and smartphones [1], [2]. If the execution time of a given task is 1ms and memory bandwidth is 10GB/s, $globalMem = 0.5M$ is the break-even point, i.e., the cost of task copying is lower for smaller copy sizes than suffering from refresh blocking. Notice that 0.5MB is larger than one I-frame of a typical MPEG stream, of which only one frame is needed roughly per 10ms at 30-60 frames/sec. Or consider two 250x250 double-precision matrices (which is less than 0.5MB) that are multiplied, with an execution time that far exceeds 1ms, i.e., no copy task would be required since the execution time exceeds 1ms so that this task's period also has to be larger than the refresh duration. Thus, we conjecture that for a real-time task with 1ms execution time and a short period in the same range, 0.5MB is quite sufficient to forward outputs of one job to the next.

Observation 5: CRS obtains better performance and higher task predictability than burst refresh of the closest prior work, and CRS can schedule short tasks which prior work cannot [3].

I. Discussion

This paper shows that the refresh overhead of a periodic real-time task set on a single processor can be hidden by our CRS. CRS could be generalized to multicore platforms under partitioned parallel scheduling of tasks with respect to cores, but the analysis would have to be revised beyond the hyperperiod as our base model [24] assumes a uniprocessor, whereas multicore schedules with task offsets may only reach a fixpoint after multiple hyperperiods [27]. Nonetheless, CRS could simply schedule the subset of tasks associated with the partition of a given core using CRS' hierarchical server model on a per-core basis, where servers receive different memory colors to guarantee when their allocated colors are not being refreshed while a server executes.

We evaluate our approach via hardware simulation, but software refresh control has been demonstrated on different hardware platforms [3], and CRS could be implemented with similar software refresh controls on such platforms (with some engineering overhead). DRAM refreshes are synchronous with the processor clock (if the clock is fixed) and can, in fact, optionally be disabled for a subset of ranks on contemporary single- and multi-core systems [28]. Furthermore, the phase when a per-rank hardware refresh starts could be reverse engineered by monitoring access latencies during the initialization of a CRS-controlled system on these platforms.